REGULATORY INFORMATION DISTRIBUTION SYSTEM (RIDS)

ACCESSION NBR:8011200178 DOC.DATE: 80/11/13 NOTARIZED: NO DOCKET #
FACIL:50-269 Oconee Nuclear Station, Unit 1, Duke Power Co. 05000269
50-270 Oconee Nuclear Station, Unit 2, Duke Power Co. 05000270
50-287 Oconee Nuclear Station, Unit 3, Duke Power Co. 05000287
AUTH.NAME AUTHOR AFFILIATION
PARKER,W.O. Duke Power Co.
RECIP.NAME RECIPIENT AFFILIATION
DENTON,H.R. Office of Nuclear Reactor Regulation, Director
REID,R.W. Operating Reactors Branch 4

SUBJECT: Forwards addl info re facility reload design methodology technical rept, in response to NRC 801016 ltr request.

DISTRIBUTION CODE: A001S COPIES RECEIVED:LTR 1 ENCL 40 SIZE: 25
TITLE: General Distribution for after Issuance of Operating License

NOTES:M Cunningham:all amends to FSAR & changes to Tech Specs. 05000269
AEOD,Ornstein:1cc.
M Cunningham:all amends to FSAR & changes to Tech Specs. 05000270
AEOD,Ornstein:1cc.
M Cunningham:all amends to FSAR & changes to Tech Specs. 05000287
AEOD,Ornstein:1cc

	RECIPIENT ID CODE/NAME		COPIES LTTR	COPIES ENCL	RECIPIENT ID CODE/NAME		COPIES LTTR	COPIES ENCL
ACTION:	REID,R.	04	13	13				
INTERNAL:	D/DIR,HUM FAC	08	1	1	I&E	06	2	2
	NRC PDR	02	1	1	OELD	11	1	0
	OR ASSESS BR	10	1	0	REG FILE	01	1	1
EXTERNAL:	ACRS	09	16	16	LPDR	03	1	1
	NSIC	05	1	1				

NOV 21 1980

TOTAL NUMBER OF COPIES REQUIRED: LTTR ~~38~~ 39 ENCL ~~36~~ 37

SL

DUKE POWER COMPANY
POWER BUILDING
422 SOUTH CHURCH STREET, CHARLOTTE, N. C. 28242

WILLIAM O. PARKER, JR.
VICE PRESIDENT
STEAM PRODUCTION

November 13, 1980

TELEPHONE: AREA 704
373-4083

Mr. Harold R. Denton, Director
Office of Nuclear Reactor Regulation
U. S. Nuclear Regulatory Commission
Washington, D. C. 20555

Attention: Mr. R. W. Reid, Chief
Operating Reactors Branch No. 4

Subject: Oconee Nuclear Station
Docket Nos. 50-269, -270, -287
Oconee Reload Design Methodology Technical Report

Dear Sir:

Your letter of October 16, 1980 requested additional information concerning the subject report. Please find attached the requested information.

Very truly yours,

William O. Parker, Jr.

FTP:scs
Attached

A001
S 1/40

ATTACHMENT

DUKE POWER COMPANY
OCONEE NUCLEAR STATION

OCONEE RELOAD DESIGN METHODOLOGY TECHNICAL REPORT

RESPONSES TO NRC QUESTIONS
OF
OCTOBER 16, 1980

Q. 1. Paragraph 3.2.5. Reactivity Coefficients and Deficits.

The described procedure for the calculation of the reactivity deficits involves PDQ07 or EPRI-NODE. However, it is not clear whether for widely different states the reactivity difference due to the spectral component is also included. The same comment applies to the differential boron worth calculation.

A. 1. The lattice code EPRI-CELL does change cross section libraries as a function of moderator temperature. These cross sections are then used in PDQ07 Version 2 for both color set calculations, which lead to input for EPRI-NODE, and for quarter core calculations. Therefore, the spectral component is included in the calculations of reactivity coefficients and reactivity deficits.

The effects of soluble boron on the flux spectrum is accounted for in two ways. First the soluble boron concentration input to the EPRI-CELL fuel depletion is varied from 1200 ppm at BOL to 400 ppm at 6000 MWD/MTU and is held constant at this concentration for the rest of the depletion. Second, the non-fuel cross sections (eg. control rod guide tubes, reflector, etc.) are generated as a function of soluble boron concentration.

Q. 2. Table 3-1, Shutdown Margin Calculation.

Give a description of the manner in which the "Worth reduction due to burnup of poison material" has been calculated.

A. 2. CPM has been used to generate a curve of control rod reactivity reduction (% $\Delta\rho$) as a function of fuel burnup at HFP Nominal conditions. This is changed to a % reduction in control rod worth versus burnup. For rodded fuel cycles the control rod bank that is inserted is conservatively assumed to have been inserted for the whole cycle. For unrodded (feed & bleed) cycles the lead regulating bank is conservatively assumed to have been inserted 20% for the whole cycle. Knowing the worth of the rod groups, the integral rod worth curve, and the accumulated burnup that each has seen, the burnup penalty can be calculated.

Q. 3. Paragraph 3.2.8, Kinetics Parameters.

Present a more detailed description of the DELAY code. Provide the source of the code, e.g., Duke Power Company.

A. 3. The DELAY code has been written by Duke Power Company. The following four pages have been extracted from the DELAY code manual and describe the theory, equations, and data sources for the code.

1.0 INTRODUCTION

DELAY is a utility type code which calculates the six group delayed neutron β's, λ's and also reduces them by a group independent effectiveness value. In addition to this, DELAY calculates the prompt neutron lifetime and then solves the In-hour equation to correlate reactivity insertion and doubling time.

Input for DELAY is available from two dimensional quarter core PDQ calculations and EPRI-CELL fuel depletion calculations.

2.0 THEORY

2.1.1 β_i, λ_i and β_i^{eff} Calculation

β_i is defined as the fraction of fission neutrons produced that appear as delayed neutrons of delayed group i. λ_i is defined as the effective decay constant for the precursors that produce delayed neutrons in delayed group i. These quantities are defined by the following equations:

$$(1) \qquad \beta_i \iint_{jg} \nu_{jg} \Sigma^F_{jg} \phi_{jg} = \iint_{jg} \beta_{ijg} \nu_{jg} \Sigma^F_{jg} \phi_{jg}$$

and

$$(2) \qquad \lambda_i \iint_{jg} C_{ijg} = \iint_{jg} \lambda_{ijg} C_{ijg}$$

where

$(\nu\Sigma^F\phi)$ is the neutron production rate, C denotes the concentration of delayed neutron precursors, and the subscripts i, j, g refer to the delayed neutron group, fissioning isotope, and incident neutron energy group respectively.

The concentration of delayed neutron precursors is related to the fission rate by

$$(3) \qquad \lambda_{ijg} C_{ijg} = k \beta_{ijg} \nu_{ijg} \Sigma^F_{ijg} \phi_{ijg}$$

Using equation 3, the solution to equations (1) and (2) becomes:

$$(4a) \qquad \beta_i = \iint_{jg} \beta_{ijg} P_{jg}$$

$$(4b) \qquad \beta_i^{effective} = \beta_i \cdot \text{EFFECTIVENESS FACTOR}$$

$$(5) \qquad \lambda_i = \frac{\beta_i}{\iint_{jg} (\beta_{ijg} P_{jg} / \lambda_{ijg})}$$

where

$$(6) \qquad P_{jg} = \frac{\nu_{jg}\Sigma^{F}_{jg}\phi_{jg}}{\sum\sum_{jg}\nu_{jg}\Sigma^{F}_{jg}\phi_{jg}}$$

is the fraction of the total neutron production rate arising from fissions of isotope j by incident neutrons of group g. Equation (6) is solved using integrated fission rate data from PDQ calculations. Suggested effectiveness factors are 0.961 for Oconee and 0.97 for McGuire.

2.1.2 Delayed Neutron Data

Tomlinson's values of delayed neutron parameters have been chosen for DELAY. The values have been reproduced here as Table I for documentation purposes and have been used in DELAY.

2.2 Prompt Neutron Lifetime

The prompt neutron lifetime, ℓ^* is defined

$$(7) \qquad \ell^* = \frac{1}{V_1\Sigma_{T1}} + \frac{k_2}{V_2\Sigma_{T2}}$$

where

$$(8) \qquad \Sigma_{T1} = \frac{\nu\Sigma_{F1}}{k_1}$$

$$(9) \qquad \Sigma_{T2} = \frac{\Sigma_{R1}}{\Sigma_{T1}} \quad \frac{\nu\Sigma_{F2}}{k_2}$$

$$(10) \qquad V_i = \frac{\sigma_a^{B-10} \text{ at 2200 m/sec}}{\sigma_{ai}^{B-10}} \times 220000 \ \frac{cm}{sec}/\frac{m}{sec}$$

The parameters and their units are defined in Table 2.

2.3 Reactivity Calculation

The In-hour equation has been simplified to include only the asymptotic reactor period. The form programmed into DELAY is the following:

$$\rho = \frac{\ell^*}{T} + \sum_{i=1}^{6} \frac{\beta_i^{\text{effective}}}{1+\lambda_i T}$$

where T = asymptotic reactor period
ρ = reactivity

TABLE 1

Delayed Neutron Data
From Tomlinson AERE-R-6993

Fast Fission

Isotope	Group	λ (sec^{-1})	± S.D.	Relative Abundance	± S.D.	Absol. Gp. Yield (n/100F)	± S.D.
U235	1	.0127	.0003	.038	.004	.063	.007
	2	.0317	.0012	.213	.007	.351	.016
	3	.115	.004	.188	.024	.310	.042
	4	.311	.012	.407	.010	.672	.034
	5	1.40	.012	.128	.012	.211	.022
	6	3.87	.548	.026	.004	.043	.007
U238	1	.0132	.0004	.013	.001	.058	.007
	2	.0321	.0009	.137	.003	.602	.037
	3	.139	.007	.162	.030	.712	.129
	4	.358	.021	.388	.018	1.708	.120
	5	1.41	.099	.225	.019	.989	.089
	6	4.02	.317	.075	.007	.330	.036
Pu239	1	.0129	.0003	.038	.004	.024	.003
	2	.0311	.0007	.280	.006	.179	.013
	3	.134	.004	.216	.027	.138	.019
	4	.331	.018	.328	.015	.210	.018
	5	1.26	.171	.103	.013	.066	.010
	6	3.21	.378	.035	.007	.022	.004
Pu240	1	.0129	.0006	.028	.004	.022	.004
	2	.0313	.0007	.273	.006	.238	.024
	3	.135	.016	.192	.079	.162	.065
	4	.333	.046	.350	.030	.315	.040
	5	1.36	.304	.128	.027	.119	.027
	6	4.04	1.16	.029	.009	.024	.007
$Pu242^{+}$	1	.0129		.004		.006	
	2	.0295		.195		.31	
	3	.131		.162		.26	
	4	.338		.411		.66	
	5	1.39		.218		.35	
	6	3.65		.010		.016	

TABLE 2

Parameters for Prompt Neutron Lifetime Calculation

Parameter	Description	Units	Source
k_1	$k_{effective}$, fast group	none	PDQ
k_2	$k_{effective}$, thermal group	none	PDQ
Σ_R	Removal cross section to thermal group	cm^{-1}	PDQ flux weighted edit fuel only
$\nu\Sigma_{F1}$	Neutron production cross section in fast group	cm^{-1}	PDQ flux weighted edit fuel only
$\nu\Sigma_{F2}$	Neutron production cross section in thermal group	cm^{-1}	PDQ flux weighted edit fuel only
Σ_{T1}	Total cross section fast group	cm^{-1}	equation 8
Σ_{T2}	Total cross section in thermal group	cm^{-1}	equation 9
V_1	Neutron velocity, fast group	cm/sec	equation 10
V_2	Neutron velocity, thermal group	cm/sec	equation 10
$\sigma_{B_{10}}(2200m)$	Thermal cross section at 2200 m/sec for B10 (3.84E+3)	barns	Chart of the Nuclides
σ_{ai}	Average boron cross section for group i	barns	PDQ
ℓ^*	Prompt neutron lifetime	sec	equation 7

Q. 4. Paragraph 8.3.2. Start-up Accident

Give the variation of the total (and its components) reactivity for the start-up accident for the first 10 seconds after the accident initiation, (these would complement Fig. 14-1 and 14-2 of the Oconee FSAR Rev 16).

A. 4. The variation of the total reactivity during a start-up accident is the sum of three reactivity effects. The withdrawal of the control rod banks adds positive reactivity which causes the neutron power level to increase and raise the average core temperature. The increase in fuel temperature causes a negative reactivity feedback due to the negative Doppler coefficient. The increase in power level increases heat transfer from the fuel to the coolant, resulting in an increase in moderator temperature. This causes a positive reactivity feedback since a positive beginning of cycle moderator coefficient is assumed. The transient response is primarily determined by the rate of positive reactivity addition from the withdrawal of rods, and the Doppler feedback which slows or terminates the nuclear excursion. The moderator feedback has a smaller effect.

The reactivity response of the startup accident simulation performed by B&W and used in the orginal FSAR analysis is not available. In order to respond to the question, the variation of the total reactivity and its components were back-calculated from the results presented in FSAR Figures 14-1 and 14-2, utilizing the analysis assumptions specified in the FSAR. Using this method, the trends of the parameters of interest can be determined with a reasonable degree of accuracy. Figures 4-1 and 4-2 show the variation of the reactivity consistent with FSAR Figures 14-1 and 14-2 respectively. It should be noted that these figures do not represent the first 10 seconds of the transients, considering that the initial conditions are 10E-9 rated power and 1% k/k subcritical. Figures 4-1 and 4-2 illustrate the time interval of greatest interest during the transient, Figure 4-1 is the same scale as Figure 14-1, and Figure 4-2 is the first one second of the response in Figure 14-2. For both transients the reactivity addition for the first 10 seconds following initiation of rod withdrawal would only cause a reduction in the subcriticality margin.

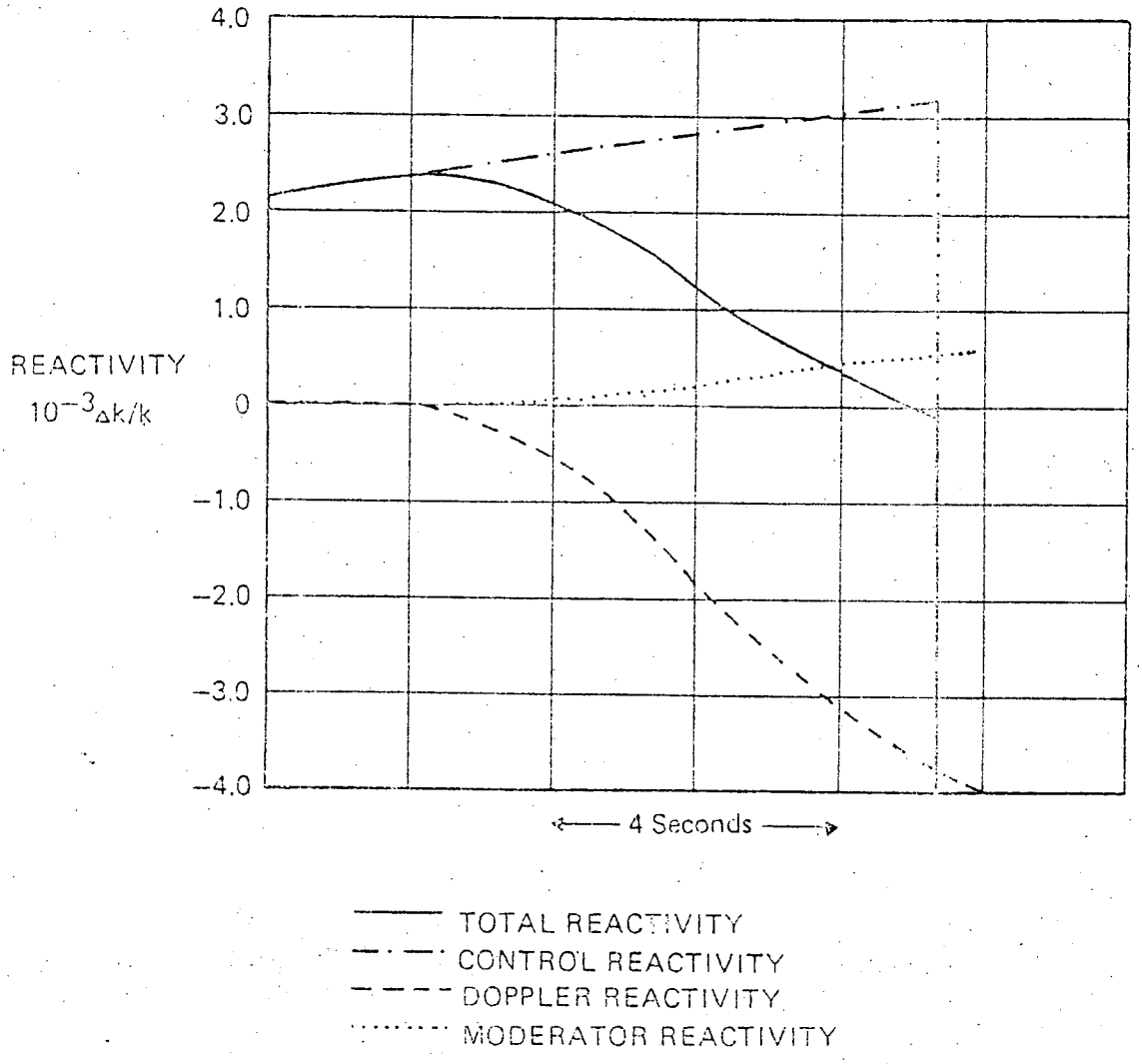

Figure 4-1. (FSAR Figure 14-1)

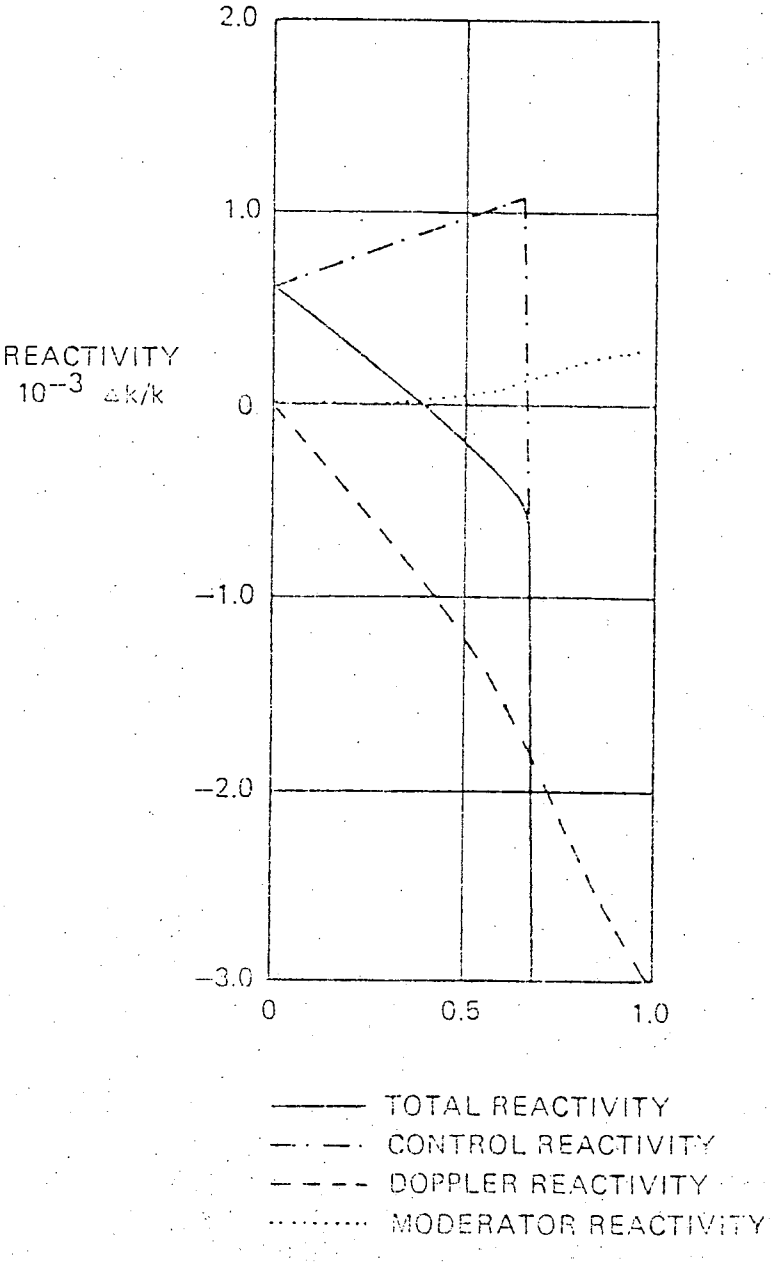

Figure 4-2. (FSAR Figure 14-2)

Q. 5. Paragraph 8.3.3. Rod Withdrawal Accident at Rated Power Operation

Give the variation of the reactivity as in 4. above.

A. 5. The reactivity response of the rod withdrawal accident at rated power simulation performed by B&W and used in the original FSAR analysis is not available. In order to respond to the question a similar analysis was performed by Duke Power Company using the RETRAN code and matching as accurately as possible the modeling assumptions of the original analysis. Figure 5-1, a revised FSAR Figure 14-9, shows the comparison between the original analysis (solid lines) and the new analysis (dashed lines). No attempt was made to match the results of the original analysis, the intent being to match the assumptions and initial conditions. The similarity between the results of the two analyses supports the conclusion that the reactivity response of the new analysis shown in Figure 5-2 is representative of the original analysis.

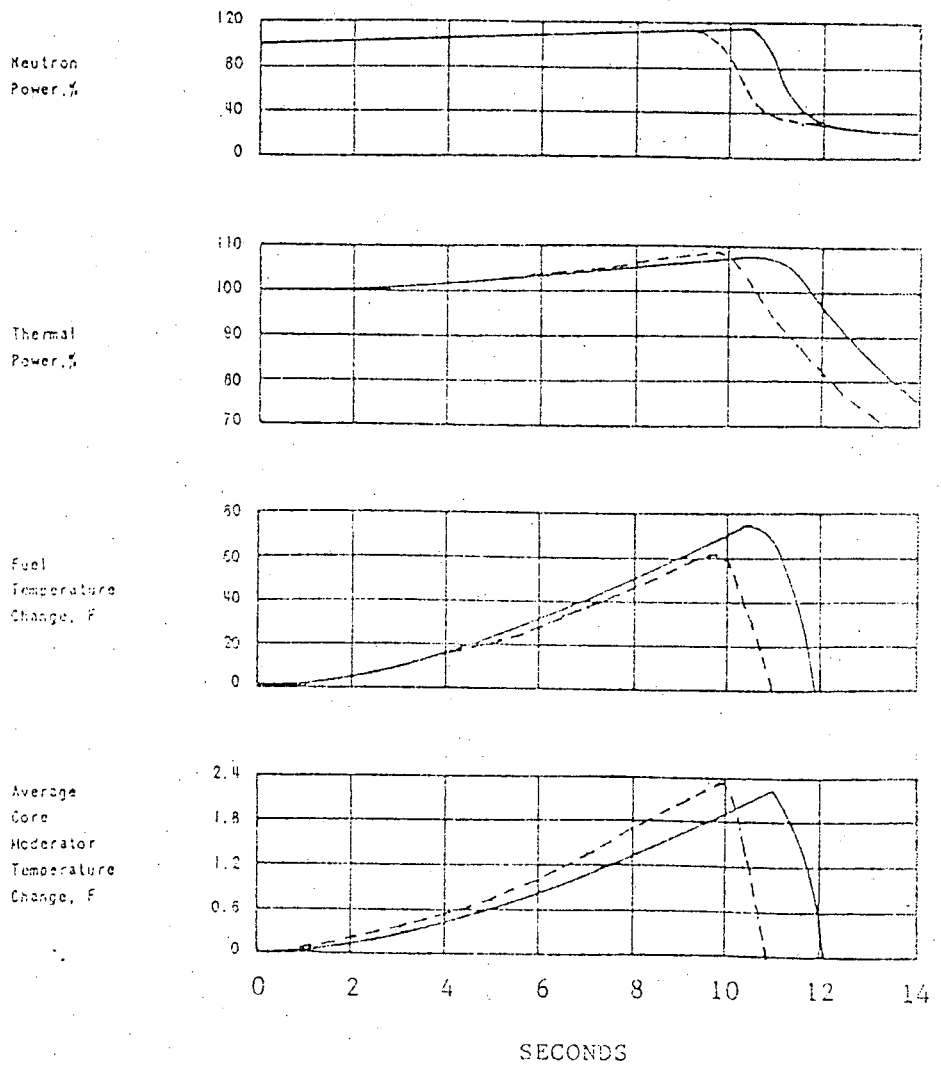

Figure 5-1 (FSAR Figure 14-9)

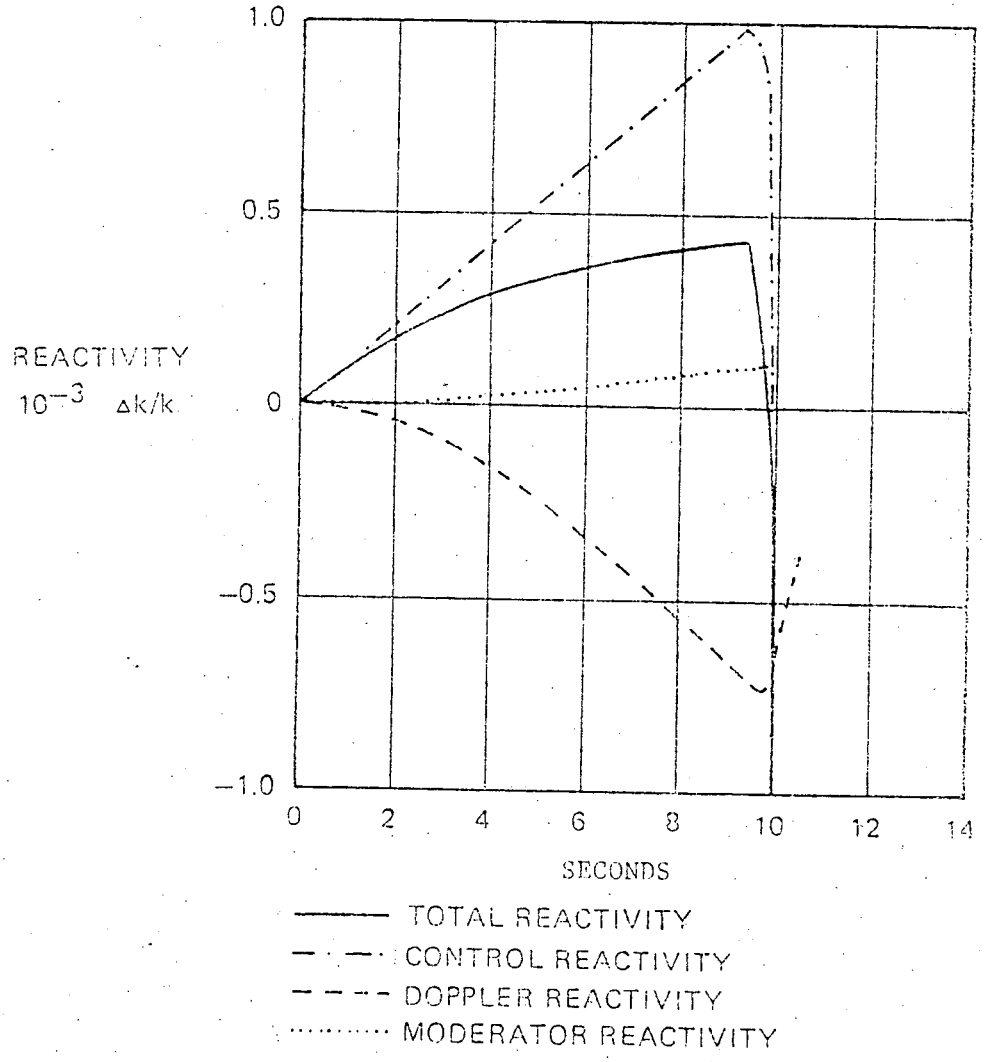

Figure 5-2 (FSAR Figure 14-9)

Q. 6. Paragraph 8.3, Discussion of Individual Accidents

Have the computer codes used in accident analysis (summarized in Appendix A) been updated and revised since the Oconee FSAR was issued? If so, would the general conclusions of the accident analysis change if the analysis was to be performed with the updated codes? Justify your conclusion.

A. 6. The computer codes summarized in Appendix A of NFS-1001 are primarily the nuclear, thermal, and thermal-hydraulic analysis codes intended for the reload core design. All the codes necessary for accident analyses are not included in that appendix.

The analysis of the loss of coolant accident was revised since the issuance of the Oconee FSAR using updated codes. BAW-10103 represents this revised analysis. Although many of the other accidents have not been reanalyzed utilizing updated codes, it is believed that the general conclusions of the existing analyses would not change if the analysis was repeated utilizing state-of-the-art computer codes. This conclusion is based on the premise that the earlier computer codes employed generally conservative modeling compared to the more accurate modeling utilized in current computer codes. Furthermore, the input parameters and assumptions employed in establishing the plant models have the dominant influence on accident consequences.

As discussed in the report, the safety analysis review performed during reload design involves a thorough review of the input data and assumptions used in the accident analyses and a comparison to the values generated by the reload design. The goal of the review is to verify that the reload design values remain bounded by the accident values and thus confirm that the safety analyses remain valid.

Q. 7. Paragraph 8.3.4. Moderator Dilution Accident

"Additional Analysis" is claimed to demonstrate complete protection during refueling operations. Give more information of this analysis.

A. 7. The "Additional Analysis" referred to is summarized in FSAR Section 14.1.2.4.2, the last paragraph on page 14-9. This paragraph is reproduced below.

During refueling or maintenance operations when the reactor closure head has been removed, the sources of dilution water makeup to the letdown storage tank--and therefore to the reactor coolant system--are locked closed, and the high pressure injection pumps are not operating. At the beginning of core life when the boron concentration is highest, the reactor is about 9.5 per cent $\Delta k/k$ subcritical with the maximum worth rod stuck out. To demonstrate the ability of the reactor to accept moderator dilution during shutdown, the consequences of accidentally filling the letdown storage tank with dilution water and starting the high pressure injection pumps have been evaluated. The entire water volume from the letdown storage tank could be pumped into the reactor coolant system (assuming only the coolant in the reactor vessel is diluted), and the reactor would still be 4.9 per cent $\Delta k/k$ subcritical.

Q. 8. Paragraph 8.3.6. Loss of Coolant Flow

It is stated that the hot channel power peak augmentation factors, fuel densification, and rod bow effects are not expected to change for the reloads; however, it is not stated how this conclusion has been arrived at.

A. 8. Hot channel power peak augmentation factors are associated with the mechanical design of the fuel assembly. The mechanical design is not normally modified in the reload design process. The fuel assembly design for Oconee has a history of very few modifications, none significantly affecting mechanical or nuclear performance. For example, the hot channel factors which account for the effect of statistical uncertainty in parameters such as enrichment, fuel rod loading, and geometry on the fuel rod heat flux and heat generation rate, remain valid for all fuel manufactured within the specified tolerances in these parameters.

The presently accepted treatment of the fuel densification effect on minimum DNBR analysis is the use of densified fuel stack length for calculating the heat flux. The original analysis was based on an initial fuel density of 92.5%, which produced the maximum stack length reduction compared to the subsequent reload fuel batches consisting of higher density fuel. For each reload, values of the densified heat flux are evaluated in the thermal hydraulic design analysis section of the reload report.

The effect of fuel rod bowing, dependent on the fuel assembly mechanical design and burnup, is explicitly factored into the thermal-hydraulic design of the reload core. The reactor protection system setpoints necessary for DNBR protection are established to provide the necessary margin to account for the effect of fuel rod bowing, as discussed in Sections 4.8 and 6.10 of NFS-1001.

Q. 9. Paragraph 8.3.9, Steam Line Failure

It is stated in the accident description that continued feedwater flow in the affected steam generator, combined with excessive heat removal and primary cool down the reactor may experience "a return to low power levels." There is not quantification of this power level, its potential consequences, or measures and actions for the return of the reactor to subcritical. Under what conditions is there a minimum of rod worth which could have the most adverse effects?

A. 9. The answers to these questions may be found in the Oconee FSAR, Chapter 14 and Supplement 3. However, a brief response summarizing the FSAR material follows.

A number of cases involving a variety of secondary system behavior during a steam line break are evaluated in the FSAR. Cases involving failure to isolate the affected steam generator, excessive feedwater addition due to malfunction in the feedwater control function, or of the auxiliary feedwater in additon to the continuing feedwater to the affected steam generator predict a return to power (1% FP, 8% FP, 35% FP, respectively) for a brief period of time. In each case, the reactor is returned to a subcritical condition by the action of the ECCS (high pressure injection, core flood tank and low pressure injection) within 350 seconds. The return to power situations are calculated to occur with the conservative assumption of the minimum tripped rod work associated with the minimum shutdown margin specified in the Technical Specifications and considering the highest-worth rod to be stuck out.

Q. 10. Supplement 2, Figure 4-1 and Paragraph 3.1.1.1.

Figure 4-1, Supplement 2 appears to contradict the statement in paragraph 3.1.1.1 that reads:

"NON-fuel cross sections with the exception of burnable poison assemblies and control rods are also generated using EPRI-CELL. Cross sections for burnable poison assemblies and control rods for use in diffusion theory calculations are generated by matching reaction rates between the diffusion theory code PDQ07 and CPM (a collision probability code)."

Give a more detailed description of the procedure for control rod and burnable poison cross section generation and the use of burnable poison cross sections in PDQ07-HARMONY depletion calculations.

A. 10. While there appears to be a contradiction both statements have merit. The ARMP procedure for generation of burnable poison cross sections was developed from CPM and PDQ07 calculations. The procedure however needs only EPRI-CELL and PDQ07 calculations to use it. Detailed description of the procedure can be found in the "Advanced Recycle Methodology Program System Documentation, September 1977." Part I Chapter 6 Section 4.2 describes the development of the procedure using CPM and PDQ07 while Section 4.3 describes the procedure using EPRI-CELL and PDQ07.

The procedure for developing control rod cross sections is described in Part I Chapter 6 Section 3.4 of the "Advanced Recycle Methodology Program System Documentation, September 1977."

Q. 11. Supplement 2, Paragraph 3.2, Comparison of ARMP PDQ07 to Cold Criticals.

The two-dimensional simulation of the cirticals has not been performed at Duke nor with PDQ07, yet it was concluded that the results would have been identical with the PDQ07 results. Justify the above conclusion.

A. 11. The cold criticals have been simulated with PDQ07. The results have been published in Part I Chapter 2, Rev. 1 of the ARMP System Documentation. This work was performed under EPRI Research Project 118-1.

These benchmark calculations use standard ARMP methodology, standard ARMP codes (EPRI-CELL, NUPUNCHER, PDQ07) and Duke Powèr also uses these codes and methodology. Therefore, if the calculations had been performed at Duke Power the results would have been identical.

Q. 12. Supplement 2, paragraph 3.4, Conclusions.

The conclusions for the calculated results of the peak power are not tenable. There is no reason why the diffusion theory estimation by PDQ07 of the local radial peaking should be more conservative than those calculated with transport theory codes, or the measured values. This result must be regarded as fortuitous. For example (Fig. 3-4), many fuel assembly maxima were underpredicted by PDQ07. Justify the conclusion that PDQ07 will always be conservative in peak power predictions and present physical arguments for this justification.

A. 12. In Section 3, PDQ07's ability to conservatively predict the assembly local radial is addressed. In Figures 3-2, 3-3, and 3-4, it was shown that the maximum local radial as calculated by PDQ07 was conservative with respect to the measured or transport theory calculated values for three completely different lattice conditions. Each of these figures show the pinwise power distributions within a single fuel assembly.

In Figures 3-2, 3, 4, the eight highest measured (or EPRI-CPM calculated) pin powers were selected. The means and standard deviations of the (calculated-measured) difference were tabulated for all three groups together, and by each group (by Figure) individually.

In these samples, the mean was taken as the sample mean with the true standard deviation unknown. Then 95% confidence limits of the true mean were determined by:

$$\bar{D}_{U,L} = \bar{D} \pm \frac{t(.025,\ n-1) * S(D)}{\sqrt{n}}$$

Table 1 displays the results of this analysis.

Table 1

95% Confidence Level Estimates of the C-M Radial Local Means

Figure	n	$\bar{D}$	S (D)	$\bar{D}_U$	$\bar{D}_L$
3-2	8	.0070	.01739	.0215	-.0075
3-3	8	.02225	.01268	.0329	.0116
3-4	8	.0105	.008767	.0178	.0032
3-2,3,4	24	.01325	.01445	.0194	.0071

A. 12. cont'd.

Since $\bar{D}>0.0$ for all four sample groups, it is concluded that PDQ07 would overpredict the mean radial local of the highest power pins within an assembly. Furthermore, using 95% confidence limits estimates, PDQ07 over-predicts the mean radial local in the lower 2.5% interval ($\bar{D}_L>0.0$) for three of the four cases considered.

Besides the observations in Chapter 3 of Supplement 2, the Oconee fuel assembly employs a uniform lattice with a small interassembly water gap. A water hole's area is only as large as that of a fuel rod so that thermal flux peaking is minimized. Likewise, even at cold conditions, the nominal water gap between assemblies is only 12% of a pin pitch.

Thermal physics constants are standardly calculated using the Mixed Number Density (MND) procedure. Thermal absorption and fission constants are products of their respective 2200 m/sec cross sections and the cell average velocity (relative to 2200 m/sec). Thermal diffusion constants are treated in a similar fashion.

Thermal reaction rates in PDQ07 are proportional to the magnitude of the thermal flux. When excess thermalization occurs, e.g., near a water hole, MND cross sections conservatively yield higher thermal reaction rates than conventional cross sections.

This conservatism of the MND method is shown in Figure 1. Here a comparison was made of MND and conventional PDQ07 pin powers relative to EPRI-CPM. The data source for the MND PDQ07 and EPRI-CPM assembly simulation was Figure 3-4 of Supplement 2. It was shown that for the eight maximum pin powers, MND cross sections yielded a mean percent difference of .99%; while the conventional cross section PDQ07 had a nonconservative mean of -.31%.

The statistics presented in Supplement 2 justify use of a radial ONRF of 1.03 for unrodded fuel cycles. We have suggested use of 1.05 which allows approximately two percent conservatism for any local pin peak uncertainties.

The above statistics, physical geometry, and modeling procedures support the conclusion that no additional uncertainty is needed on the radial local peak. However, a 2% conservatism is built into the 1.05 radial ONRF we propose using.

A.12

FIGURE 1

PERCENT DIFFERENCE COMPARISON OF PIN POWERS

REFERENCE CALCULATION: EPRI-CPM

CODE USED	PDQ07	PDQ07	EPRI-CPM
MODEL	1/4 ASS'Y	1/4 ASS'Y	1/4 ASS'Y
X-SECTIONS	MND	CONV	CPM
%FP	100	100	100
PPMB	0.0	0.0	0.0

IT							
-.79 -1.58	.29 -.59	MND PDQ07 CONV PDQ07					
-.30 -.10	0.0 ⑥ -.96						
-.40 .20	.98 .69	.85 ② -.38	2.45 ⑤ .94				
-.40 .40	.98 .79	1.04 ③ -.28	1.76 ① -.19				
-.30 .30	.10 ⑧ -.58		1.13 ④ -.56	.58 ⑦ -.48	.41 .41		
-.82 .21	.30 .40	-.29 -.78	.60 .50	-.21 .41	-.84 .21	-1.28 0.0	
-1.25 .10	-.94 .21	-.52 .41	-.73 .31	-1.05 .21	-1.38 0.0	-1.61 -.11	-1.52 -.11

*NOTE: PIN #1 IS THE PEAK LOCAL RADIAL, #2 - THE SECOND HIGHEST PIN, ETC.

Q. 13. Supplement 2, paragraph 4.2, Oconee Fuel Cycle Simulation.

It appears that the EPRI-NODE-P almost consistently under-predicts the assembly peak power for cycles 2 and 3. Justify the conclusion in paragraph 4.3 that the EPRI-NODE-P "yielded consistently good power distributions..."

A. 13. Conclusions about power distributions are reached in view of the global behavior of EPRI-NODE-P. The Cycle 3 data was shown in Section 4 of Supplement 2 only for illustrative purposes since the measured data was not considered benchmark quality as the other four cycles.

The derived total ONRF from chapter 5 was 1.10 for rodded cycles. Only 6% of the products of the ONRF and calculated peak exceeded the cycle 2 measured peaks. Therefore, based on a 95/95 criterion, the agreement was judged good.

Q. 14. Supplement 2, Figure 4-2 through 4-127.

The EPRI-NODE-P calculated power distributions for the first four cycles of operation of Oconee 1 consistently underpredicted the relative power in assembly H-8, often by more than 10%. Is the reason for this anomaly known?

A. 14. Yes. It is current Duke design practice to perform only one radial power normalization at approximately 25 EFPD. The normalization is referenced to a two-dimensional discrete pin model PDQ07 power distribution.

The normalization is performed such that there is good radial power agreement in both the central nine (H-8 included) and the peripheral assembly regions. Since only the internal leakage factor, g_h, was adjusted for the central nine, agreement of the central nine as a whole was addressed rather H-8 specifically. This method yielded radial differences of 5% or less early in each cycle for H-8 as shown by Figures 4-4, 4-41, and 4-87. Assembly K-9 in Cycle 3 had a 20% larger radial at BOC than H-8, therefore the central nine normalization gave a more accurate agreement with a more limiting assembly. Cycles 1, 2, and 3 were all rodded cycles, and therefore rod interchanges severely changed the radial power shape. A radial power renormalization to PDQ07 after the rod interchange would have significantly improved radial and peak agreement.

The reactors at Oconee will soon all be operated in the unrodded mode and so only the statistics for Cycles 4 and 5 are representative of future design calculations.

In Cycle 4, the largest radial power difference for H-8 was 3.3%. In Cycle 5, differences of up to 10% were seen. However, H-8 was a low power assembly, and K-9 was the assembly of concern. Good agreement was shown between assemblies K-9 and also H-9 throughout this cycle.

The only other method of assuring less than 5% power difference to H-8 would have been to apply a K_∞ multiplier. Such an ad hoc method of normalization is contrary to Duke design practice.

Q. 15. Supplement 2, paragraph 5.2, Normality Test Results.

All data sets have been used with the assumption of normal distribution, yet some have failed the normality test. Justify the use of the data sets as normal.

A. 15. The D' test for normality is a very rigorous test, and in Table 5-1 of Supplement 2 it was shown that nine of 16 individual and grouped data sets passed the normality criteria outright - with a 5% level of significance.

Table 1 below presents the percent differences by which the other seven data sets missed the D' percentage point cutoff values for normality. Of these seven, four data sets were combinations of individual nonnormal datasets which in turn, carried inherent near-normality into the larger sets.

Table I

Nearly Normal Data Sets

Cycle	Type	N	Percent Difference from Cutoff	Figure
1	Radial	308	-2.16%	5-11
1,2	Radial	455	-1.75%	5-21
1,2,4,5	Radial	730	-1.56%	5-23
1	Peak	377	- .26%	5-16
3	Peak	211	-3.67%	5-19
1,2	Peak	612	-1.38%	5-24
1,2,4,5	Peak	1027	-1.72%	5-26

The argument presented in paragraph 5.2 was that although certain distributions did not pass the normality test criteria, an ocular inspection of the histograms indicated that, for engineering purposes, normality would be a reasonable approximation of these distributions. This is further supported by Table I above.

It should also be noted that cycle 4, cycle 5, and cycle 4 & 5 radial and peak power data sets passed the normality test. These unrodded cycles are typical of future Oconee reload designs.